Dynamics of the second-order nonlinearity in thermally poled silica glass

D. Faccio,[a] V. Pruneri, and P. G. Kazansky
Optoelectronics Research Centre, Southampton University, Southampton, SO17 1BJ, United Kingdom

(Received 2 October 2000; accepted for publication 25 June 2001)

We study the temporal evolution of both the second-order nonlinear coefficient and of the nonlinear thickness in thermally poled silica-glass slides by using a high-resolution all-optical technique. A time delay in the nonlinearity formation is observed, followed by an increase to a maximum, and a final decrease. The thickness is shown to increase at a rate that differs significantly from that reported for the corresponding ionic charge fronts. Our measurements also show strong dependencies on sample thickness and these can be attributed to different electric fields in the depletion region. © *2001 American Institute of Physics.* [DOI: 10.1063/1.1394948]

Ever since its first demonstration,[1] thermal poling as a means of inducing a second-order nonlinearity (SON) in glass has attracted much interest due to its potential applications in various optical devices. The results obtained are highly reproducible and, although the SON is small compared to other nonlinear materials (e.g., $LiNbO_3$), the figure of merit of poled fibers is high enough to justify this interest, e.g., for frequency conversion of high-power fiber lasers[2] and generation of correlated parametric photons.[3] It is a well-established fact that in glass the mechanism at the basis of SON formation is ionic migration and subsequent creation of a frozen-in internal electric field.[1,4] However, theoretical modeling of field-assisted ion migration is rather complex and has been limited to one[5] or two species,[6] whereas experimental evaluation of positive-ion movement[7] may not be sufficient to determine the exact internal electric-field profile. In this article, we investigate the temporal evolution of the nonlinear coefficient (d_{33}) and of the nonlinear thickness (L) in thermally poled silica using the noncollinear Makers fringe technique (NCMFT), which allows high resolution.[8]

In order to study the nonlinearity evolution, samples of different thicknesses (S) were thermally poled for various poling times. The silica-glass samples were Herasil 1 grade (from Heraeus) with $S=1$, 0.5, and 0.1 mm. Thermal poling was performed at 270 °C in air by applying a constant voltage (V) of 4 kV, using Al-evaporated electrodes, for seven different times (t): 2, 5, 10, 20, 30, 45, and 90 min. The samples were subsequently cooled to room temperature with the voltage still applied. Cooling from 270 to 200 °C (when poling effects become negligible) takes ~40 s.

The nonlinear depth was obtained using the NCMFT, which allows nondestructive measurements of thicknesses as small as 2 μm with submicron resolution.[8] Two identical input fundamental beams are focused onto the sample with a relative 90° external angle. The power of the generated noncollinear second-harmonic (SH) beam is measured as a function of the sample inclination angle and L is estimated by fitting the spacing and position of the observed peaks with the function given in Ref. 8. The measurements were carried out using a Q-switched and mode-locked Nd:YAG laser as the fundamental source. A half-wave plate controls the polarization of the fundamental pulses before they are split by a 50% beamsplitter and focused onto the sample. The SH signal was measured with a photomultiplier tube after eliminating the fundamental beam using broadband and interferometric filters. Figure 1 shows an example of the SH power as a function of inclination angle for a sample with $S=0.5$ mm and poled for 10 min, along with the best fit obtained assuming a truncated-Gaussian nonlinear profile $\propto s(L)\exp[-(z-L/4)^2/L^2]$, where $s(z)=1$ if $0<z<L$ and is otherwise null and in this particular case $L=3.4$ μm, as shown in the inset of Fig. 1. The sharp decrease in the profile may be due to the presence of a thin charge layer.[9,10] Once L is known the nonlinear coefficient is found by normalizing the collinear SH with respect to that from a reference sample (quartz) and assuming that the tensorial components of the nonlinearity d_{33} and d_{31} are related to each other by $d_{33}=3d_{31}$. All measurements were made 1 h after poling and then repeated a week later without observing any significant variation in the measured L or d values. Figure 2 shows the observed evolution of the nonlinear coefficient d_{33}. A fast initial increase is followed by a significant decrease to a final value which is roughly 50% smaller than the peak d_{33}. Furthermore, the poling times for which the peak d_{33} values are observed decrease with decreasing S.

The main mechanism for the nonlinearity formation is thought to be electric-field-induced ion migration[4]—after cooling the sample and removing the electrodes an electric field (E) remains frozen in the sample that couples with the third-order nonlinearity to give an effective SON.

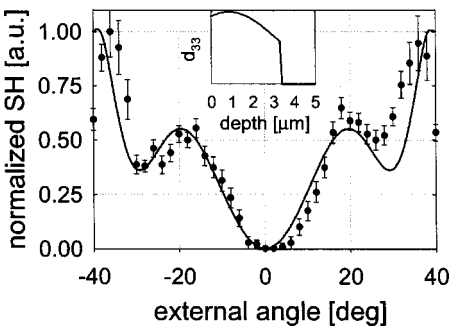

FIG. 1. Example of the noncollinear Makers fringe measurement on a 0.5-mm-thick Herasil 1 sample thermally poled at 280 °C, 4 kV, 10 min. Circles, experimental data; solid line, best fit obtained using $L=3.4$ μm.

[a]Electronic mail: dfaf@orc.soton.ac.uk

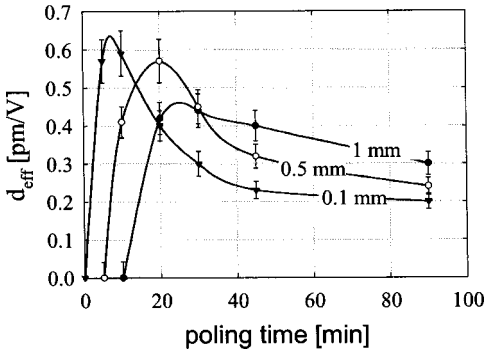

FIG. 2. Experimental values for the nonlinear coefficient (d_{33}) against poling time for samples of different thicknesses (S): $S=1$ mm, full circles; $S=0.5$ mm, open circles; $S=0.1$ mm, full triangles. The lines are only a guide for the eye.

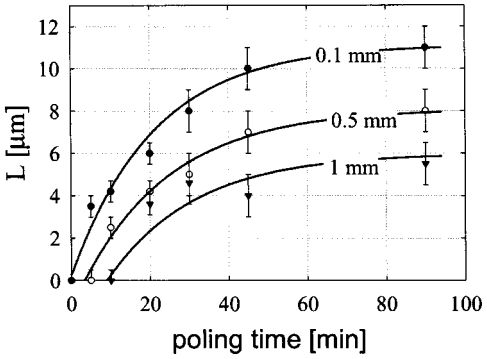

FIG. 3. Experimental values for the nonlinear thickness (L) against poling time for samples of different thicknesses (S): $S=0.1$ mm, full circles; $S=0.5$ mm, open circles; $S=1$ mm, full triangles. The lines are the best-stretched-exponential fits for the experimental data.

$$d_{33}=\tfrac{3}{2}\chi^{(3)}E, \tag{1}$$

where $\chi^{(3)}$ is the glass third-order nonlinear susceptibility and E is the frozen-in electric field. The full equations which describe this process, considering both drift and diffusion, can be rather complicated and have been solved under simplified conditions. Von Hippel[5] considered only one ion species drifting which, in our case, would be sodium (Na^+), the main charge carrier in silica glass[11] with mobility μ_{Na}. As the thermally mobilized ions drift towards the cathode, two distinct regions form in the glass: a depleted region with negative space charge followed by an undepleted, neutral region. The depletion region forms under the anode with a monotonically increasing depth, until the equilibrium value $L_\infty=\sqrt{2\epsilon V/\rho}$ is reached (where ϵ is the glass dielectric constant and ρ the depleted charge density). The internal voltage drop also increases with t and the overall effect is an increase in the frozen-in electric field, i.e., in d_{33}, and the maximum value is reached at equilibrium. Therefore, a one-charge carrier model cannot account for our experimental results which show a fast growth to a maximum followed by a slower decrease to smaller values.

The next most mobile charge carrier in silica glass is H^+,[11] with a mobility (μ_H) which has been found to be in the range 10^{-4}–10^{-3} μ_{Na}.[12,13] If press-contact or non-blocking evaporated electrodes are used, then hydrogen continuously diffuses under the influence of the externally applied electric field from the external atmosphere into the glass.[11,12,14] Due to the fact that $\mu_H \ll \mu_{Na}$, three regions will form: straight under the anode a region with Na^+ substituted by H^+—the charge in this region will depend on the amount of in-diffused H^+. This is followed by a negatively charged depletion layer, and finally by the undepleted neutral region. It is worth noting at this point that this model is still an approximation of the true situation. Indeed, the Na^+-depleted region is very different from the untreated glass: the most mobile charge carriers have been removed and an electric field close to dielectric breakdown value is applied. Under these conditions a non-Ohmic electronic current is to be expected. However, in its simplicity, the as-described two-charge carrier model provides valuable insight to thermal poling.

The equations describing the process have been solved by Alley, Brueck, and Myers—[6] the electric field inside the sample initially rises but is then followed, for longer poling times, by a decrease to smaller values. The nonlinear coefficient, proportional to the electric field, will follow the same evolution. It is worth noting that the above model describes thermal poling in air: poling in vacuum or with blocking electrodes shows a different behavior.[6,15] As we were able to ascertain using a similar model, the poling times for which the maximum d_{33} values are obtained depend on many parameters, such as ion concentrations and mobilities which vary from glass to glass. Most importantly, there is a strong dependence on S due to the higher electric-field values inside the thinner samples, thus explaining the results in Fig. 2 where we show the nonlinear coefficient against poling time. Figure 2 also shows that there seems to be a minimum poling time below which no nonlinearity is observed (also observed in Ref. 6). This minimum poling time is smaller than 40 s (necessary to apply the voltage and cool the sample) for $S=0.1$ mm, but increases to 5 min for $S=0.5$ mm and to 10 min for $S=1$ mm. Furthermore, poling at a higher temperature (e.g., 280 °C) resulted in a shift of these threshold times to smaller values (2 min for $S=0.5$ mm and 5 min for $S=1$ mm). These results may be explained by assuming that the time required for a charge distribution to form, such that SH generation (SHG) can occur, depends on both temperature and sample thickness (maybe due to a reduced mixed-ion mobility near the cathode[6]). By raising the temperature (i.e., ionic mobility) or decreasing the sample thickness (i.e., increasing the applied electric field), the necessary charge distributions are achieved for smaller poling times.

Figure 3 shows the evolution of L for the same samples of Fig. 2. The well-known continuous increase in L is observed (see, e.g., Ref. 15). The lines show the best fits for functions of the form

$$L(t)=L(0)+\alpha(1-e^{-\beta t}), \tag{2}$$

where $L(0)+\alpha=L(\infty)$ is the saturation value and β is the growth rate. The values which gave the best fits for L are shown in Table I. β_L is the same for all S, indicating that the nonlinearity-formation mechanism is the same for all sample thicknesses. $L(0)$ is a fictitious quantity due to the absence of a SH signal for small t as already discussed—in fact, for small t we are still uncertain if $L\to 0$ very rapidly or if the nonlinearity starts to form over a finite thickness. For larger t, all experimental L values are well described by Eq. (2). However, the observed evolution of L differs (in particular,

TABLE I. Values for the parameters $L(0)$, α, and β used in the fitting function $L(0)+\alpha(1-e^{-\beta t})$ for L for all three sample thicknesses (S).

$S\rightarrow$	1 mm	0.5 mm	0.1 mm
$L(0)$ (μm)	−3.1	−1.26	0
α_L (μm)	9	9.39	10.87
β_L (min^{-1})	0.045	0.044	0.046

for $S=0.1$ mm) from the measured positive ion-charge front evolution [$\propto \ln(t)$],[6,16] implying that the actual value of the nonlinear thickness may not correspond to that expected from these measurements. It is well known that a depletion region a few microns thick forms in the first seconds of poling,[7] but we may infer from our measurements that another mechanism (maybe electronic migration) is necessary in order to also observe SHG and to explain the differences between positive-charge-distribution and SH measurements. Figure 3 also shows a marked dependence on sample thickness which may be qualitatively assigned to the different electric fields inside the samples.

Figure 4 shows the product $d_{33}L$ against poling time. The growth rates vary according to the sample thickness but the saturation value is roughly the same ($\simeq 2.4\times10^{-18}$ m^2/V) for all S. This value may be used to estimate the $\chi^{(3)}$ using Eq. (1) and assuming that all the applied 4 kV voltage drops across the depletion region and remains constant. In this case we find $\chi^{(3)}=4\times10^{-22}$ m^2/V^2, in good agreement with values estimated by other means.[17,18]

In conclusion we have measured the evolution for small poling times of nonlinear thickness L and of the second-order nonlinear coefficient d_{33} in thermally poled silica glass using an all-optical characterization technique. Our results differ substantially from those obtained on the basis of positive charge migration in silica, implying that other factors must be taken into account, e.g., electronic conduction. The results show that while L increases monotonically, d_{33} reaches a maximum value for short ($\simeq$10–20 min) poling times and then decreases. On the other hand, the product $d_{33}L$ reaches a constant equilibrium value for short poling times and has been used to estimate the glass $\chi^{(3)}$. We have also reported a dependence of the measured quantities on sample thickness which can be ascribed to the different internal electric fields in the depletion region. These results are useful to optimize the efficiency of the SON in waveguide devices where the overlap between the nonlinear and waveguiding regions, along with the d_{33} optimization, is of major importance.

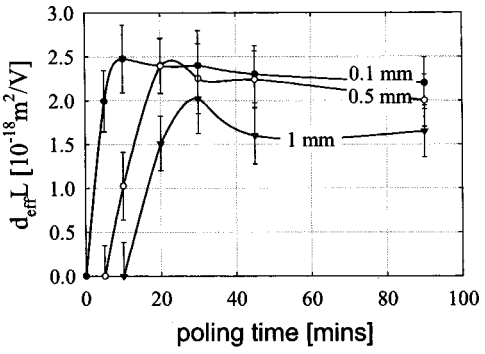

FIG. 4. Product $d_{33}L$ of the measured nonlinear coefficient and thickness against poling time for three sample thicknesses: $S=0.1$ mm, full circles; $S=0.5$ mm, open circles; $S=1$ mm, full triangles. The lines are only a guide for the eye.

This research was supported by Pirelli Cables and Systems.

[1] R. A. Myers, N. Mukherjee, and S. R. J. Brueck, Opt. Lett. **16**, 1732 (1991).
[2] V. Pruneri, G. Bonfrate, P. G. Kazansky, D. J. Richardson, N. G. Broderick, J. P. deSandro, C. Sommineau, P. Vidakovic, and J. A. Levenson, Opt. Lett. **24**, 208 (1999).
[3] G. Bonfrate, V. Pruneri, P. G. Kazansky, P. Tapster, and J. G. Rarity, Appl. Phys. Lett. **75**, 2356 (1999).
[4] P. G. Kazansky and P. St. J. Russell, Opt. Commun. **110**, 611 (1994).
[5] A. von Hippel, Phys. Rev. **91**, 568 (1953).
[6] T. G. Alley, S. R. J. Brueck, and R. A. Myers, J. Non-Cryst. Solids **242**, 165 (1998).
[7] T. G. Alley, S. R. J. Brueck, and M. Wiedenbeck, J. Appl. Phys. **86**, 6634 (1999).
[8] D. Faccio, V. Pruneri, and P. G. Kazansky, Opt. Lett. **25**, 1376 (2000).
[9] A. L. C. Triques, C. M. B. Cordiero, V. Balestrieri, B. Lesche, W. Margulis, and I. C. S. Carvalho, Appl. Phys. Lett. **76**, 2496 (2000).
[10] P. G. Kazansky, A. R. Smith, P. St. J. Russell, G. M. Yang, and G. M. Sessler, Appl. Phys. Lett. **68**, 269 (1996).
[11] U. K. Krieger and W. A. Lanford, J. Non-Cryst. Solids **102**, 50 (1988).
[12] W. A. Lanford, K. Davis, P. Lamarche, R. Groleau, and R. H. Doremus, J. Non-Cryst. Solids **33**, 249 (1979).
[13] G. Hetherington, K. H. Jack, and M. W. Ramsay, Phys. Chem. Glasses **6**, 6 (1965).
[14] P. J. Jorgensen and F. J. Norton, Phys. Chem. Glasses **10**, 23 (1969).
[15] V. Pruneri, F. Samoggia, G. Bonfrate, P. G. Kazansky, and G. M. Yang, Appl. Phys. Lett. **74**, 2423 (1999).
[16] T. G. Alley and S. R. J. Brueck, Opt. Lett. **23**, 1170 (1998).
[17] P. G. K. Kazansky and V. Pruneri, in Conference on Bragg Gratings, Photosensitivity, and Fiber Optics, No. BTuC6-1, 305 (1997).
[18] D. Wong, W. Xu, S. Fleming, M. Janos, and K. M. Lo, Opt. Fiber Technol.: Mater., Devices Syst. **5**, 235 (1999).